

SHEAR STRESS PROFILE IN A ROTATING CAGE

Prabhu Ramachandran
Department of Aerospace Engineering
IIT Bombay
Mumbai
INDIA 400076

Sunder Ramachandran, Michael Greaves, and Vladimir Jovancicevic
Baker Petrolite
12645 W. Airport Blvd.
Sugar Land, TX 77478

ABSTRACT

The rotating cage apparatus is used in the oil and gas industry as a test to recreate corrosion situations under high shear conditions. Recent work has been done by one of the authors to study the unsteady fluid dynamics of this apparatus as an idealized two-dimensional problem and perform high resolution simulations of the rotating cage using a vortex method. This work will be extended to help corrosion scientists to understand how the variation of drag coefficient profiles as a function of Reynolds number changes with coupon configuration. Drag coefficient profiles will also be computed for a rotating cage configuration that uses 2 coupons in the rotating cage as contrasted with 4 coupons in the rotating cage. This work provides new results for the drag coefficient at higher Reynolds numbers and compares the drag coefficient of rotating cages that use either 2 or 4 coupons. The drag coefficient results along the coupon profile explain extensive corrosion seen at both leading and trailing edges of the coupons in actual corrosion experiments.

Keywords: flow induced corrosion, vortex method, fluid mechanics, carbon dioxide corrosion

INTRODUCTION

The rotating cage apparatus has been used extensively by many workers to study flow induced corrosion and evaluate the ability of corrosion inhibitors to withstand the effects of high shear corrosion.¹⁻³ The rotating cage apparatus has been used to test corrosion inhibitors for the oil and gas industry.^{2,3} Corrosion inhibitors that were selected with these tests have been in use in demanding applications for several years.^{2,3} The flow and shear stress profile of the rotating cage is more complex than the rotating cylinder electrode⁴ or the jet impingement device⁵ making the interpretation of results using the rotating cage apparatus more complex. In this work, new results are presented on the fluid mechanics of the rotating cage apparatus as computed using the Random Vortex Method (RVM). The findings presented herein expand upon earlier results⁶ with this method for a higher range of Reynolds number and also incorporates the effect of using 2 or 4 corrosion coupons.

APPARATUS AND NUMERICAL PROCEDURES

A sketch of the apparatus is provided in Figure 1. The dimensions used in the work are similar to those of the earlier work and are shown in Figure 2.

Two non dimensional numbers used to characterize the flow are the Reynolds number, Re , and drag coefficient, C_f . The non-dimensional numbers are used to make the simulation applicable for different dimensions with the same geometry and configuration. In this work the Reynolds number of flow, Re , for this system is defined in equation (1).^{6,7}

$$Re = \frac{\Omega R_c^2}{\nu} \quad (1)$$

In equation (1), Ω is the angular velocity, R_c is the radial distance to the coupon, while ν is the kinematic viscosity of the fluid. The Reynolds number is a ratio of inertial forces to viscous forces.

The drag coefficient, C_f , for this system is defined by the following equation (2).⁷

$$C_f = \frac{\tau}{0.5\rho\Omega^2 R_c^2} \quad (2)$$

In equation (2), ρ is the density of the fluid and τ is the shear stress. The drag coefficient is a non-dimensional measure for shear stress.

The fluid mechanics of the rotating cage is calculated using the Random Vortex Method.^{6,8-11} The method solves the Navier–Stokes equation for an incompressible fluid in 2 dimensions. The solution is for unsteady flow and hence directly incorporates the effect of turbulence. However, it must be noted that the simulations are two-dimensional and thus do not capture any three dimensional effects. The method and its application to the rotating cage problem is described in details in previous work.⁶

RESULTS

Drag Coefficient as a Function of Length

The variation of drag coefficient on the outer surface of the coupon as a function of non-dimensional distance (x/L) from the leading edge for the 4 coupon case is shown in Figure 3. The drag coefficient is directly proportional to shear stress. The simulations show that the drag coefficient and shear stress are highest at the leading edge of the coupon as would be suggested by boundary layer theory for a flat plate.^{7,12} Not unexpectedly, corrosion damage is seen in experiments to be most severe at the leading edge.³ Another feature that is seen from the simulation is an increase in drag coefficient and shear stress at the trailing edge. This feature is not anticipated by boundary layer theory but is seen in actual corrosion coupons.³

The drag coefficient profile as a function of non-dimensional distance (x/L) from the leading edge of the coupon on the inner coupon surface along the length of the coupon is shown in Figure 4. This figure is also for the 4 coupon case. As was described in previous work, the profile obtained by these simulations is more similar to flow of a flat plate at a slight angle of attack rather than flow over a rotating cylinder.⁶ The simulations show the difference in drag coefficient or shear stress at the leading and trailing edge of the coupon. It also shows the difference in drag coefficient and shear stress between the inner and outer surface. For mass transfer limited corrosion, areas of higher shear stress will experience higher corrosion rates.

Dependence of Average Drag Coefficient and Maximum Drag Coefficient with Reynolds Number

The variation of the average drag coefficient on the coupon with Reynolds number for the outer and inner surfaces is shown for the two coupon case in Figure 5. The variation is in accordance with the vorticity and velocity field results in previous work⁶ that indicate a transition in the pattern of turbulence between a Reynolds number of 20,000 and 40,000. Figures 6a, 6b, and 6c plot the vorticity and velocity vectors for the 2 coupon case at $Re=10000$, 50000 and 200000 respectively. The variation seen is similar to that reported earlier⁶. It is clear that there is a qualitative difference in the flow beyond $Re=10000$.

The variation of the maximum drag coefficient on the coupon (for the 2 coupon case) with Reynolds number is shown in Figure 7. This quantity is more important for corrosion studies as it characterizes the highest shear stresses seen in the experiment. Whenever corrosion rates are mass transfer limited, the areas with higher drag coefficient or shear stress will experience higher corrosion rates.

Comparison of Drag Coefficients With Systems using 2 or 4 Coupons in the Rotating Cage

Simulations were also performed on a rotating cage that contained 2 coupons and the result was contrasted with the simulations that contain 4 coupons in the rotating cage. The variation of average drag coefficient on the upper surface for both 2 coupon and 4 coupon configurations as a function of Reynolds number in the rotating cage is shown in Figure 8. It can be seen from this graph that the 2 coupon configuration has higher drag coefficients.

The variation of average drag coefficient with Reynolds number on the lower surface for both the 2 coupon and 4 coupon configuration is shown in Figure 9. Again the 2 coupon configuration has higher drag coefficients than the 4 coupon configuration.

The patterns are similar with maximum drag coefficient. The variation of the maximum drag coefficient on the upper surface with Reynolds number for both 2 coupon and 4 coupon configurations is shown in Figure 10. The variation of the maximum drag coefficient with Reynolds number on the lower surface for both 2 and 4 coupon configurations in the rotating cage is shown in Figure 11. It can be seen here that the maximum drag coefficient is consistently higher with the 2 coupon configurations at all Reynolds numbers. The maximum drag coefficient is of greatest interest when one is attempting to recreate conditions in which flow induced corrosion occurs in the field.

DISCUSSION AND CONCLUSIONS

The rotating cage apparatus has often been used in studies that attempt to simulate the conditions in which flow induced corrosion occurs.¹⁻³ Interpretation of the results has been more complicated due to the complex fluid mechanics of the system. In order to develop better methods for corrosion protection, it is important that laboratory tests recreate conditions seen under field conditions as accurately as possible. It is also important to be able to understand the relevance of the test methodology with the chemistry and physics seen in oil field conditions.

The Random Vortex Method was used to understand the fluid mechanics of the system. Application of this method has shown that the flow pattern in the rotating cage is more similar to flow of a flat plane at slight angle of attack rather than flow over a rotating cylinder.⁴ The drag coefficient as a function of length showed that the largest values of drag coefficient or shear stress are seen at the leading edge. As one proceeds along the coupon the drag coefficient decreases. Interestingly, the drag coefficient increases again right at the trailing edge of the coupon. The pattern of drag coefficient dependence with coupon length is similar to the corrosion pattern seen in tests using the rotating cage.³ Simpler approaches in understanding the shear stress profile in the rotating cage^{1,12} did not explain these patterns. This is the first theoretical approach that explains this pattern. The simulations showed differences in the drag coefficient obtained in rotating cages with 2 or 4 coupons in the rotating cage.

The present results are preliminary and form a small but important advancement on previous work.⁶ There remain a number of issues that require further clarification. Some of the smaller issues relate to changes in geometry of the system. In this work, the change from 2 to 4 coupon configurations was examined. In future work, it is planned to compare the results of a full unsteady fluid dynamics simulation in 2 dimensions with one in three dimensions to see how three dimensional effects may change the nature of turbulence in this complex system.

REFERENCES

1. Schmitt, G. and Bakalli, M.; 2006 “A critical review of measuring techniques for corrosion rates under flow conditions”, Paper No. 593, CORROSION 2006, NACE International
2. Ramachandran, S., Ahn, Y. S., Greaves, M., Jovancicevic, V., Bassett, J.; 2006 “Development of high temperature, high pressure corrosion inhibitor”, Paper No. 377, CORROSION 2006 NACE International
3. Ramachandran, S., Mancuso, S., Bartrip, K. A., Hammonds, P. 2006 “Inhibition of acid gas corrosion in pipelines using glycol for hydrate inhibition”, Paper No. 477, CORROSION 2006 NACE International
4. Silverman, D. C.; 2004 “The Rotating Cylinder Electrode for Examining Velocity- Sensitive Corrosion – A Review”, Corrosion, Vol 60, No.11, pg 1003 -1023.
5. Chin, D. T. and Tsang, C. H.; 1978 “ Mass Transfer to an Impinging Jet Electrode”, Journal of Electrochemical Society, Vol. 125, No. 9 pg 1461-1470.
6. Ramachandran, P.; 2006 “Numerical Simulation of the Rotating Cage Problem”, Proceedings of 33rd National and 3rd International Conference on Fluid Mechanics and Fluid Power, Paper No. 1202, December 7-9, 2006, IIT Bombay, India.
7. Bird, R. B., Stewart, W. E., Lightfoot, E. N., “Transport Phenomena” , John Wiley & Sons, 1960 (pg. 142- 146 , Example 4.4.2).
8. Chorin, A. J.; 1973 “Numerical simulation of slightly viscous flow”, Journal of Fluid Mechanics, Vol 57. No. 4 pg. 785-796.
9. Chorin, A. J.; 1978 “Vortex Sheet Approximation of boundary layers”, Journal of Computational Physics, Vol 27. No. 3 pg. 428-442.
10. Puckett, E. G.; 1991 “Vortex methods: An introduction and survey of selected research topics” In *Incompressible Computational Fluid Dynamics – Trends and Advances*, R. A. Nicolaides and M. D. Gunzburger Eds. Cambridge University Press pg. 335.
11. Ramachandran, P.; 2004 *Development and Study of a high resolution two-dimensional vortex method* Ph D. Thesis, Department of Aerospace Engineering, IIT-Madras.
12. Dougherty, J. A.; Ramachandran, S.; and Short, B.; 1991 “Does shear stress have an effect on corrosion in sour gas production”, Paper No. 01069, CORROSION 2001

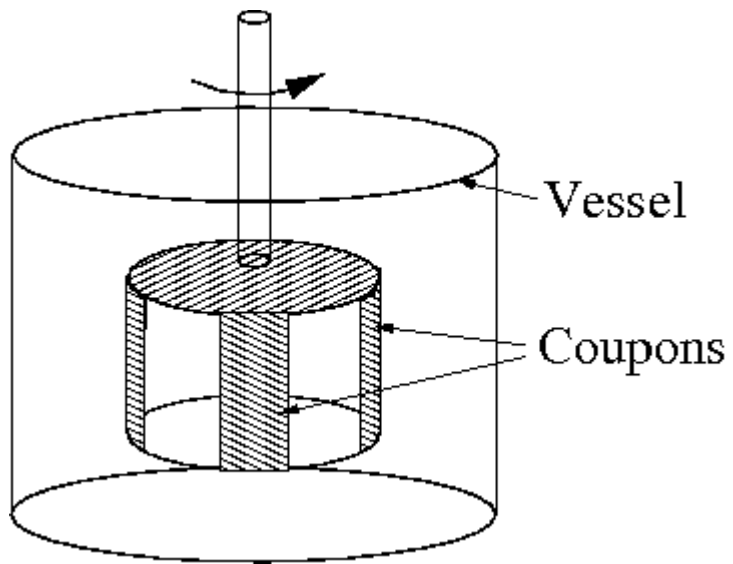


FIGURE 1. Sketch of the rotating cage apparatus.

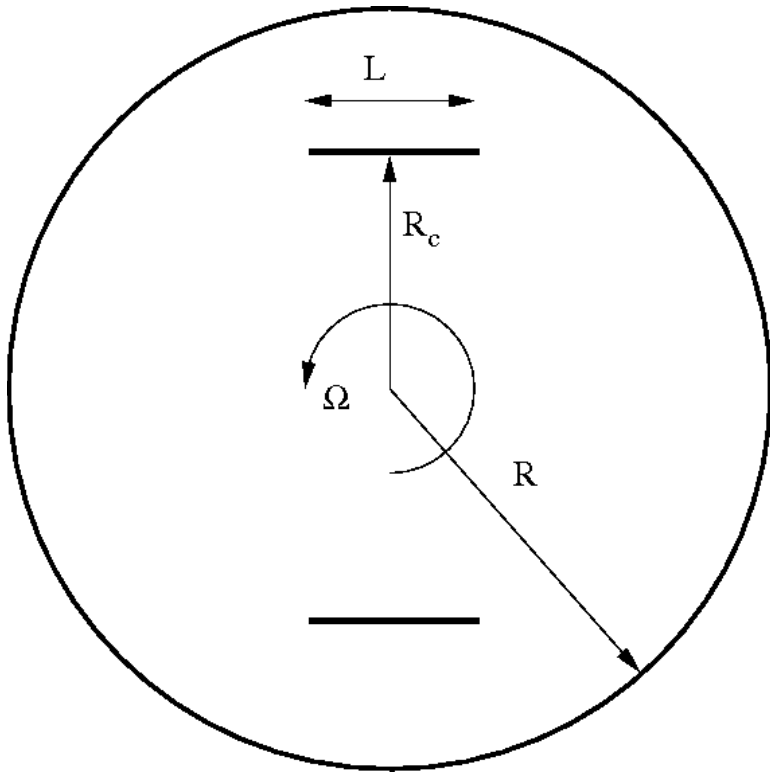


FIGURE 2. Illustration of the 2D problem being solved along with the various parameters involved.

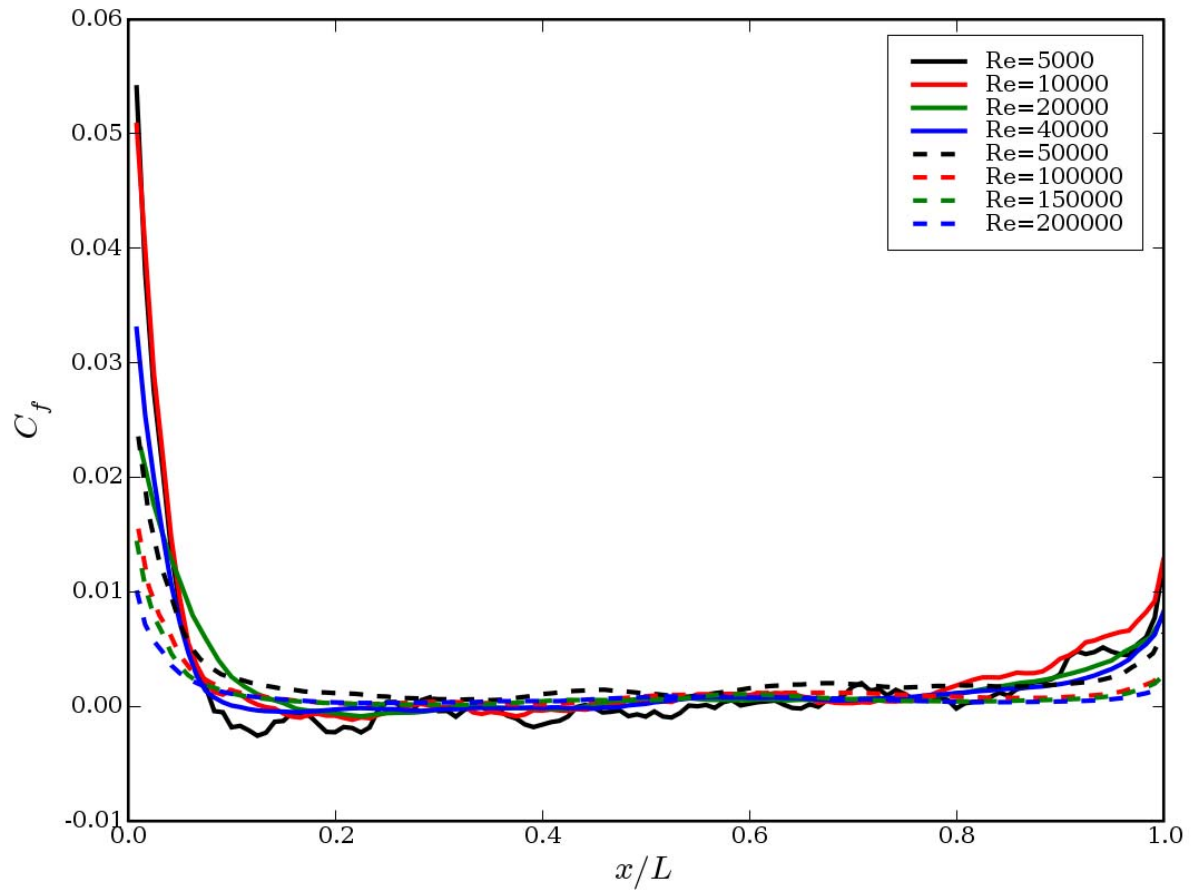


FIGURE 3. Variation of drag coefficient as a function along the length of the coupon for the outer surface for the 4 coupon case.

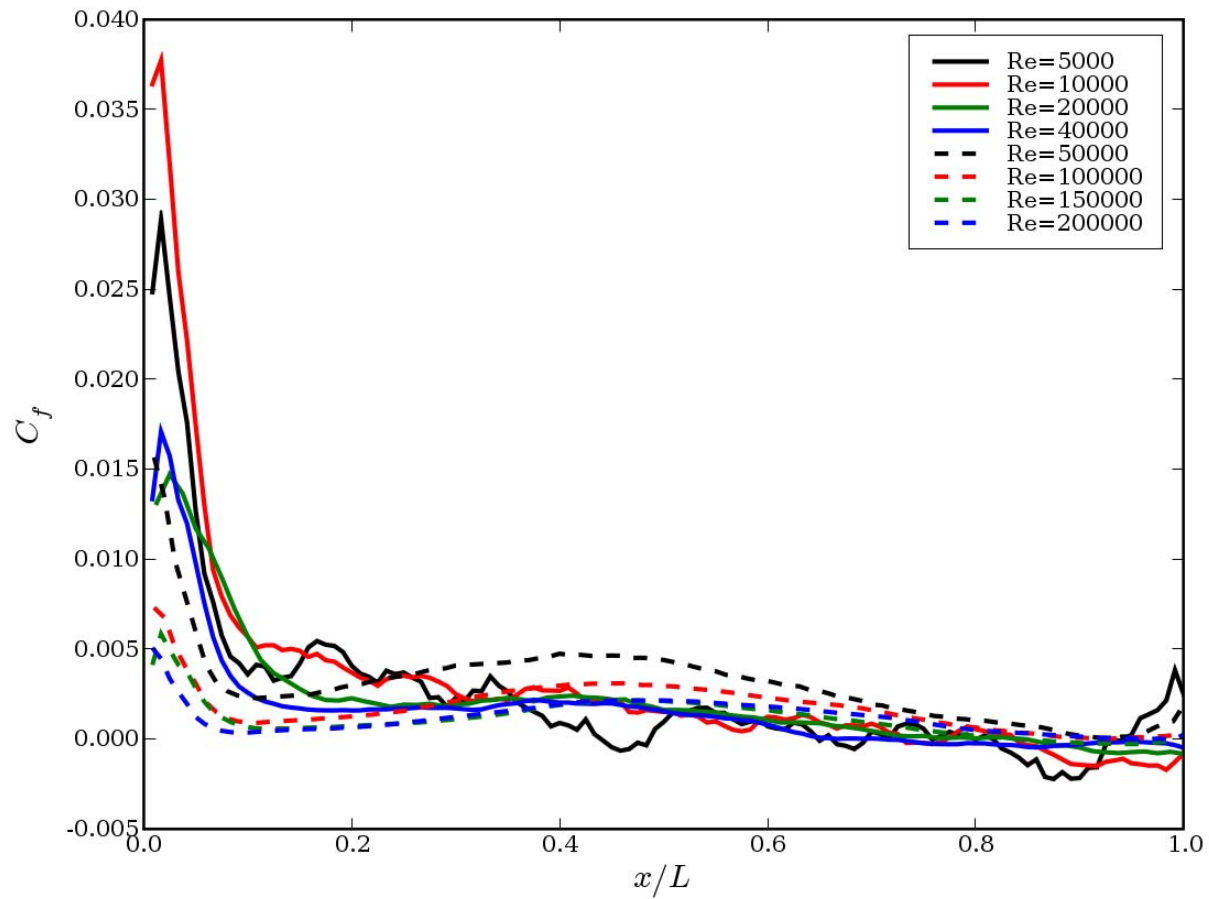


FIGURE 4. Variation of drag coefficient as a function along the length of the coupon's inner surface for the 4 coupon case.

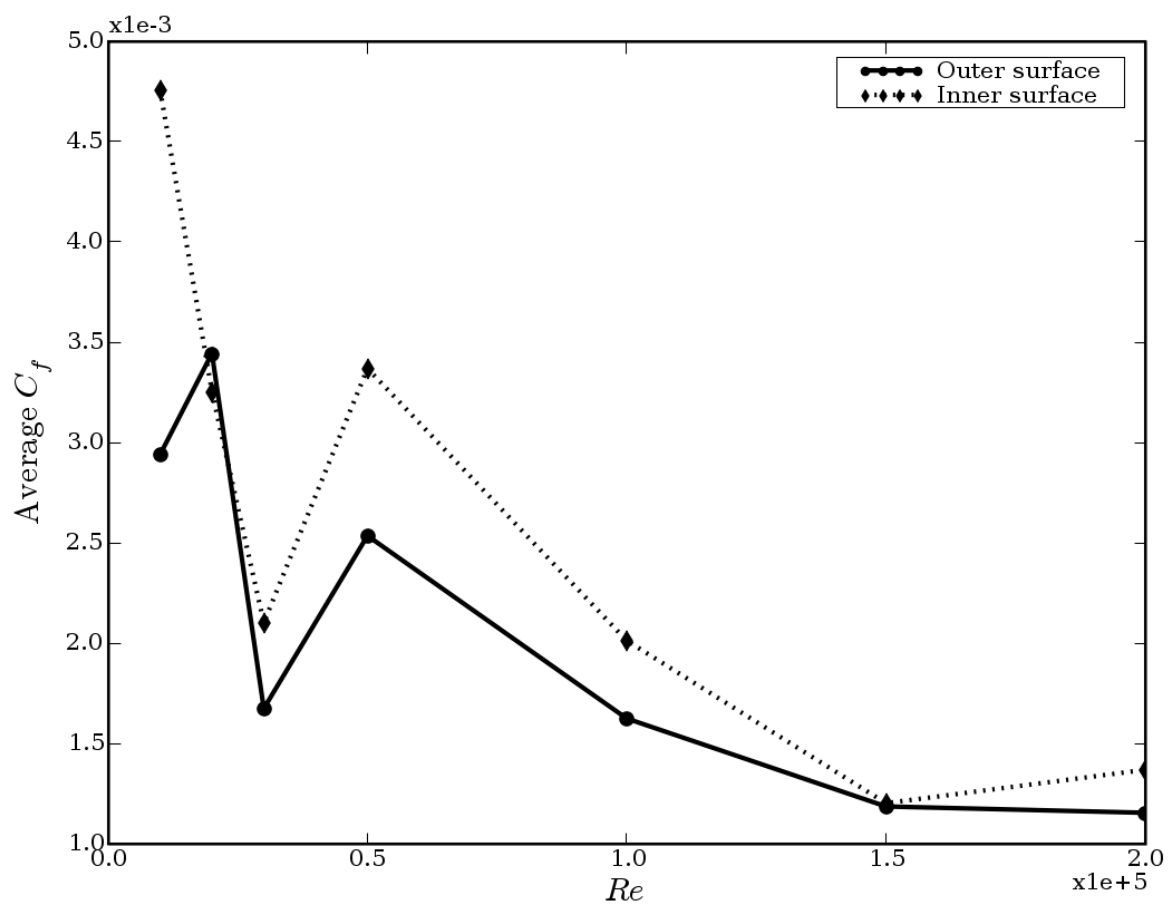


FIGURE 5. Variation of average drag coefficient on Reynolds number for the outer and inner surfaces of the 2 coupon case

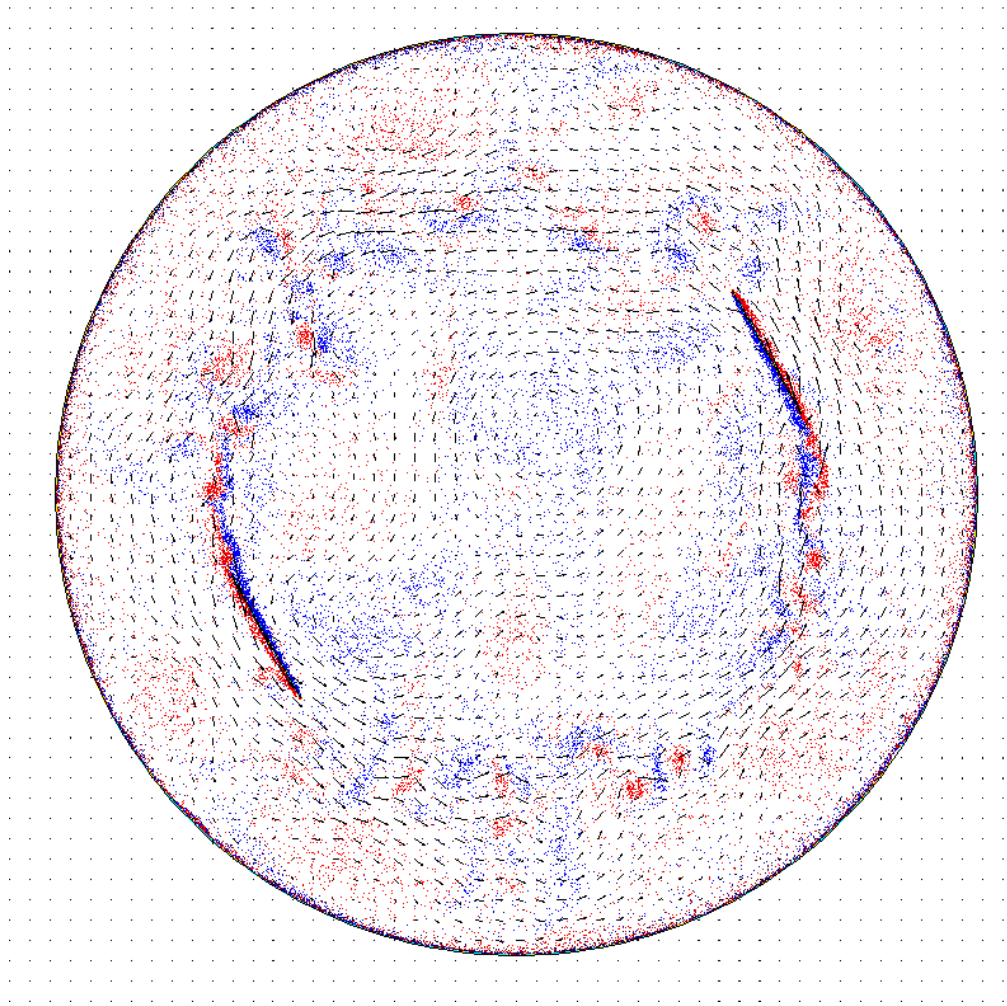


FIGURE 6a. Vorticity and velocity vectors at $Re=10000$ for the 2 coupon case. Red dots indicate clockwise vorticity and blue indicates counter-clockwise vorticity.

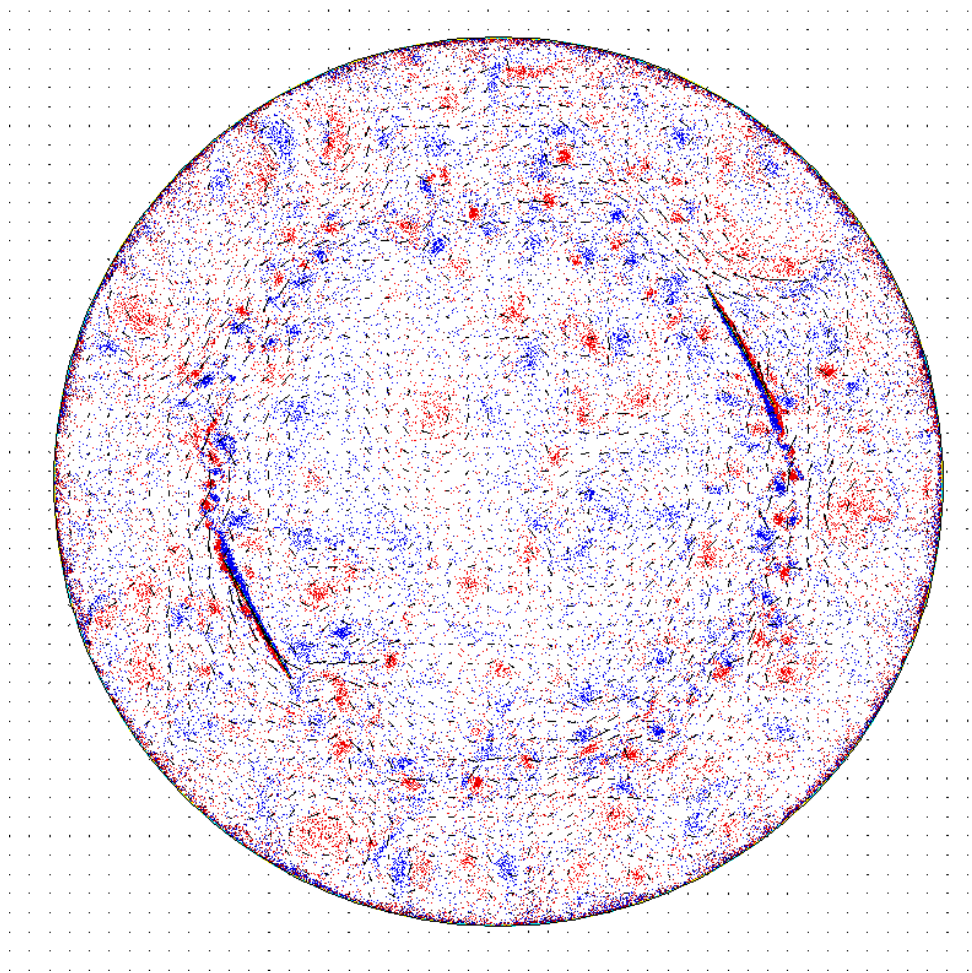


FIGURE 6b. Vorticity and velocity vectors at $Re=50000$ for the 2 coupon case. Red dots indicate clockwise vorticity and blue indicates counter-clockwise vorticity.

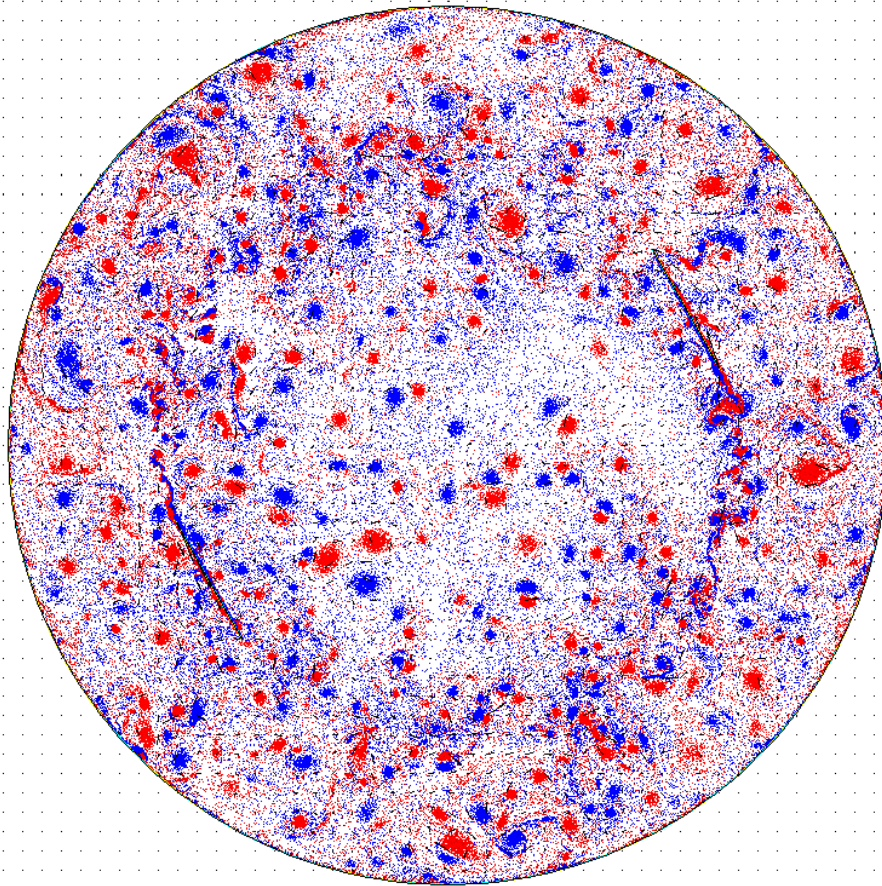


FIGURE 6c. Vorticity and velocity vectors at $Re=200000$ for the 2 coupon case. Red dots indicate clockwise vorticity and blue indicates counter-clockwise vorticity.

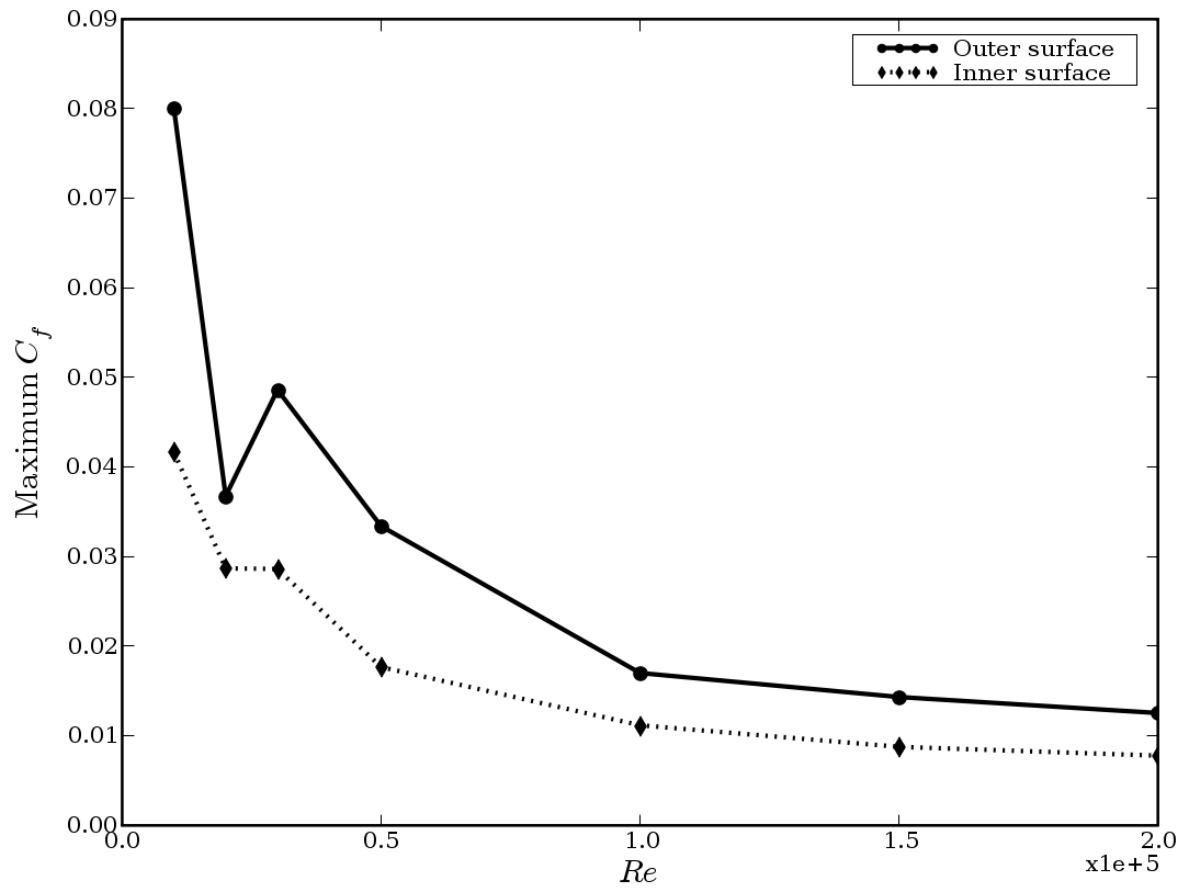


FIGURE 7. Variation of maximum drag coefficient on Reynolds number for the outer and inner surfaces for the 2 coupon case.

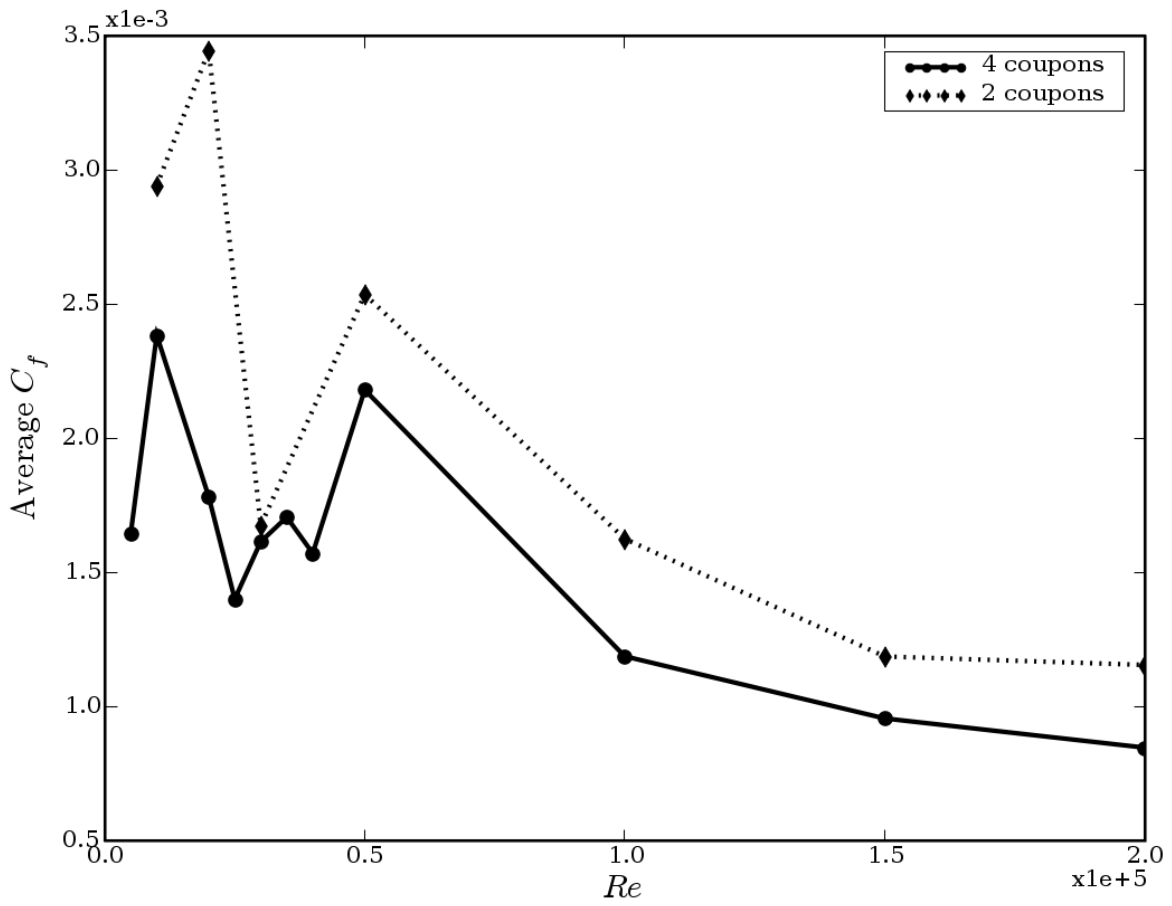


FIGURE 8. Comparison of average drag coefficient on outer surface for 2 coupon and 4 coupon rotating cage configurations.

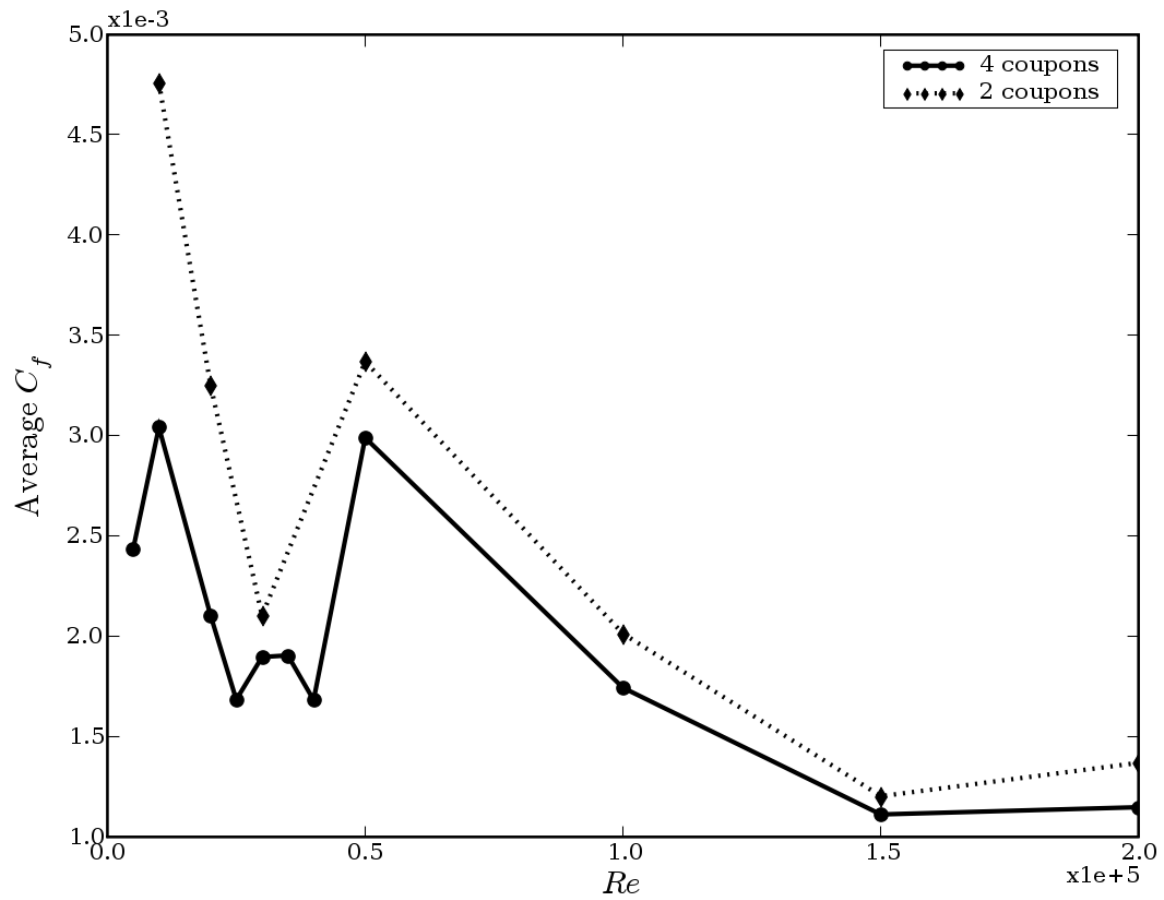


FIGURE 9. Comparison of average drag coefficient on inner surface for 2 coupon and 4 coupon rotating cage configurations

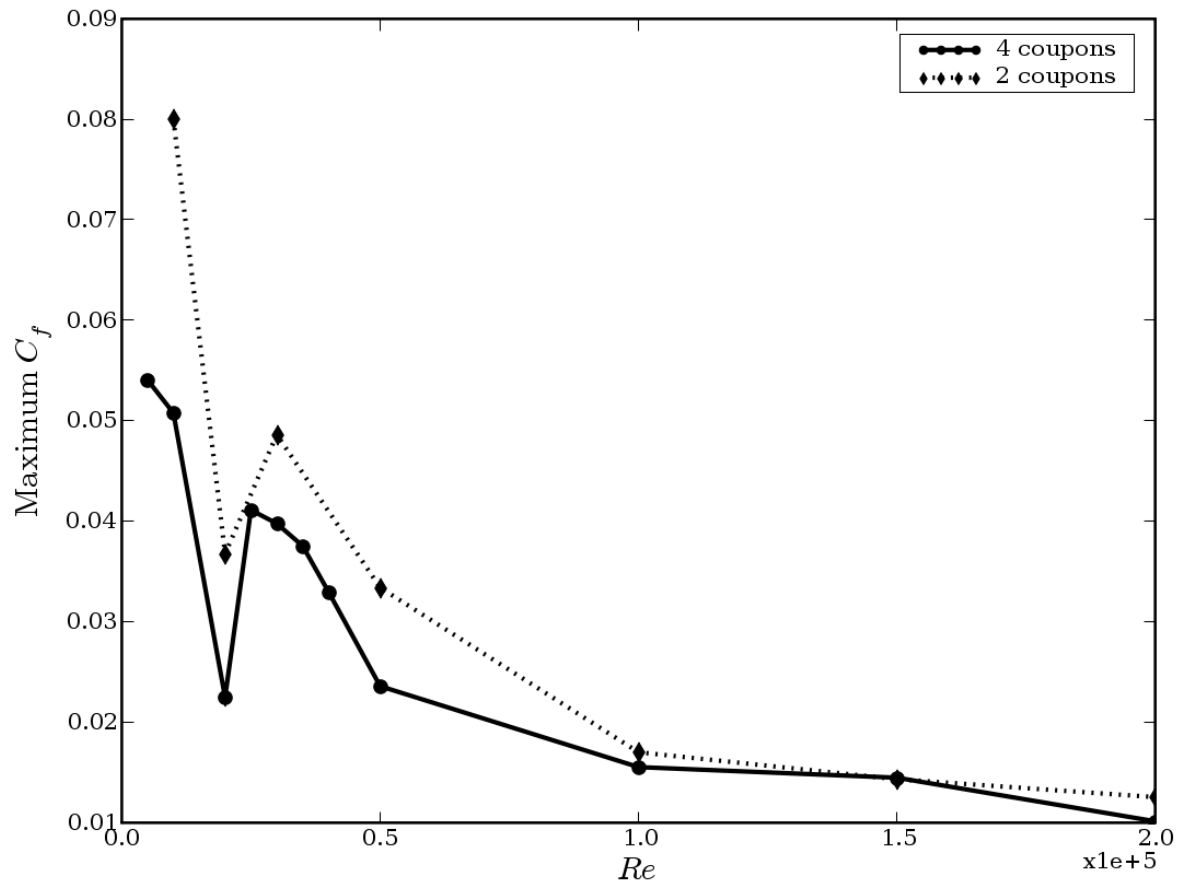


FIGURE 10. Comparison of maximum drag coefficient on outer surface for 2 coupon and 4 coupon rotating cage configurations

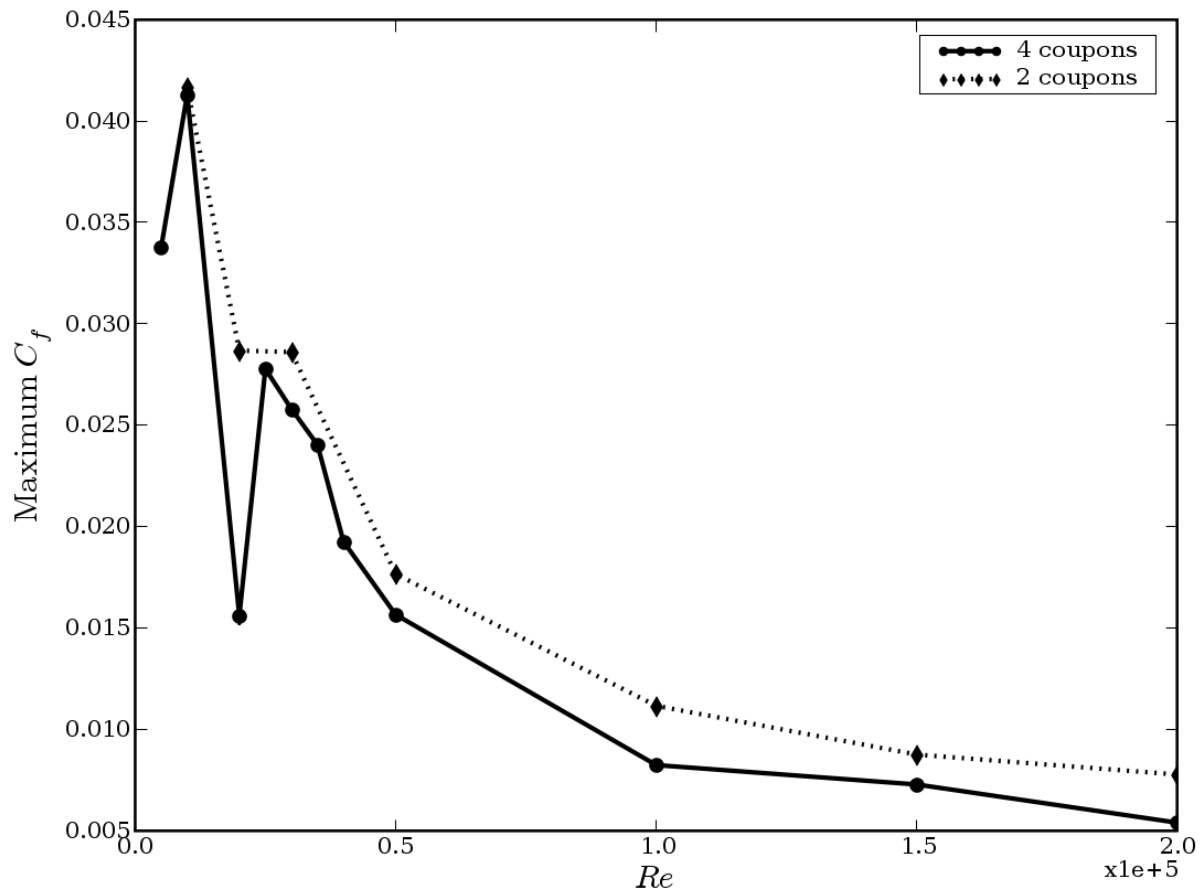


FIGURE 11. Comparison of maximum drag coefficient on inner surface for 2 coupon and 4 coupon rotating cage configurations